

Sequential assimilation of multi-mission dynamical topography into a global finite-element ocean model

S. Skachko (1), T. Janjić(2), S. Danilov (2), J. Schröter (2), D. Sidorenko (2), R. Savcenko (3) and W. Bosch (3)



(1) Département des Sciences de la Terre et de l'Atmosphère Université du Québec à Montréal, Montréal Canada (skachko.sergey@uqam.ca), (2) Alfred Wegener Institute for Polar and Marine Research, Bremerhaven, Germany, (3) Deutsches Geodätisches Forschungsinstitut, Munich, Germany.

1 Introduction

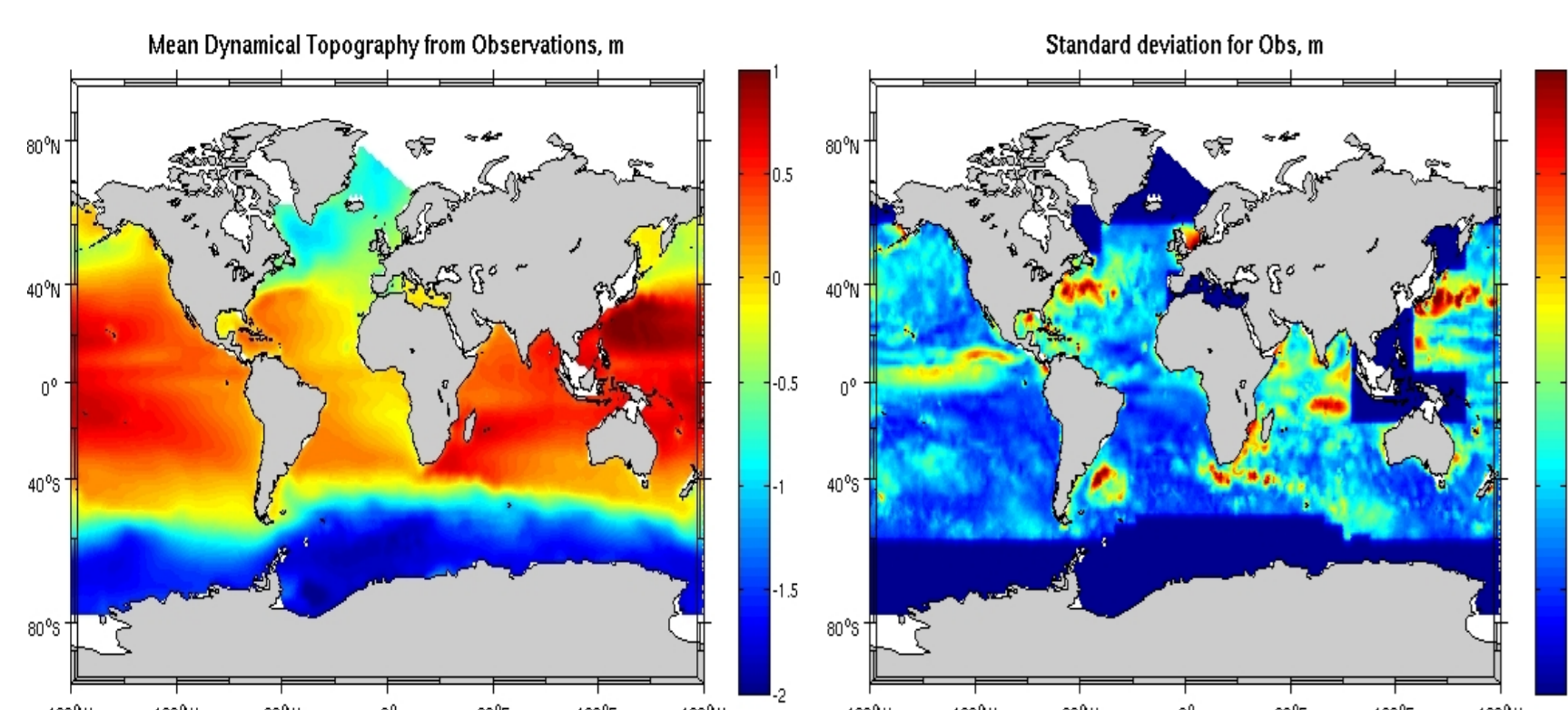
This study focuses on an estimation of ocean circulation via assimilation of satellite measurements of dynamical ocean topography (DOT) into the global finite-element ocean model (FEOM). The DOT data are derived from a complex analysis of multi-mission altimetry data combined with a referenced earth geoid. The goal of this work is exploring the feasibility of assimilation of the global altimetric signal based on sequential assimilation technique. Two different sequential assimilation techniques were implemented.

First technique uses the method of adiabatic correction [7, 2] to reduce systematic difference between mean state of the model and the mean DOT. Then, a local SEIK filter (as implemented within PDAF [6]) is used for the assimilation of the time varying DOT and temperature and salinity are updated following the vertical structure of the first baroclinic mode. Second sequential technique uses the local SEIK filter without adiabatic corrections for all model fields while assimilating the same data.

2 Observations

The DOT data were provided by R. Savcenko and W. Bosch, DFG, Munich, Germany. They were obtained by combining the ENVISAT, GFO, Jason and TOPEX/Poseidon missions data with a referenced geoid provided by the Geo-Forschung Zentrum (GFZ), Potsdam, Germany. The data cover the period between January 2004 and January 2005. They are interpolated onto the model grid so that the observations are available at every point of the model grid every ten days.

The presence of ice makes the altimetry data unusable in the polar areas. The Indonesian region is characterized by complex bottom topography where neither geoid measurements nor model results appear to be accurate enough. This is also true for the Mediterranean Sea. The observational data in these areas were substituted by the values of the RIO05 mean dynamical topography (MDT). These areas are shown in the right panel of figure below as the deep-blue rectangular areas.



Left: The mean DOT for the period from January 2004 till January 2005.

Right: Standard deviation for the same time period. The deep-blue rectangular areas correspond to the locations where the RIO05 MDT was substituted in the data (no variability).

3 Ocean model

The study was performed by the Finite-Element Ocean circulation Model (FEOM) [4, 1] configured on a global almost regular triangular mesh with the spatial resolution of 1.5° . There are 24 unevenly spaced levels in the vertical direction. The model is forced at the surface with momentum fluxes derived from the ERS scatterometer wind stresses complemented by TAO derived stresses and relaxed to monthly mean climatology at the surface. It is initialized by mean climatological temperature and salinity. This configuration is further referred to as V_1 .

4 Comparison of model results with observations

After a 10-year spin up from the state of rest, versions V_1 is run for one additional year and the output is stored every 10 days. The left panel of the figure below depicts the difference between the mean DOT and the mean calculated from V_1 model run.

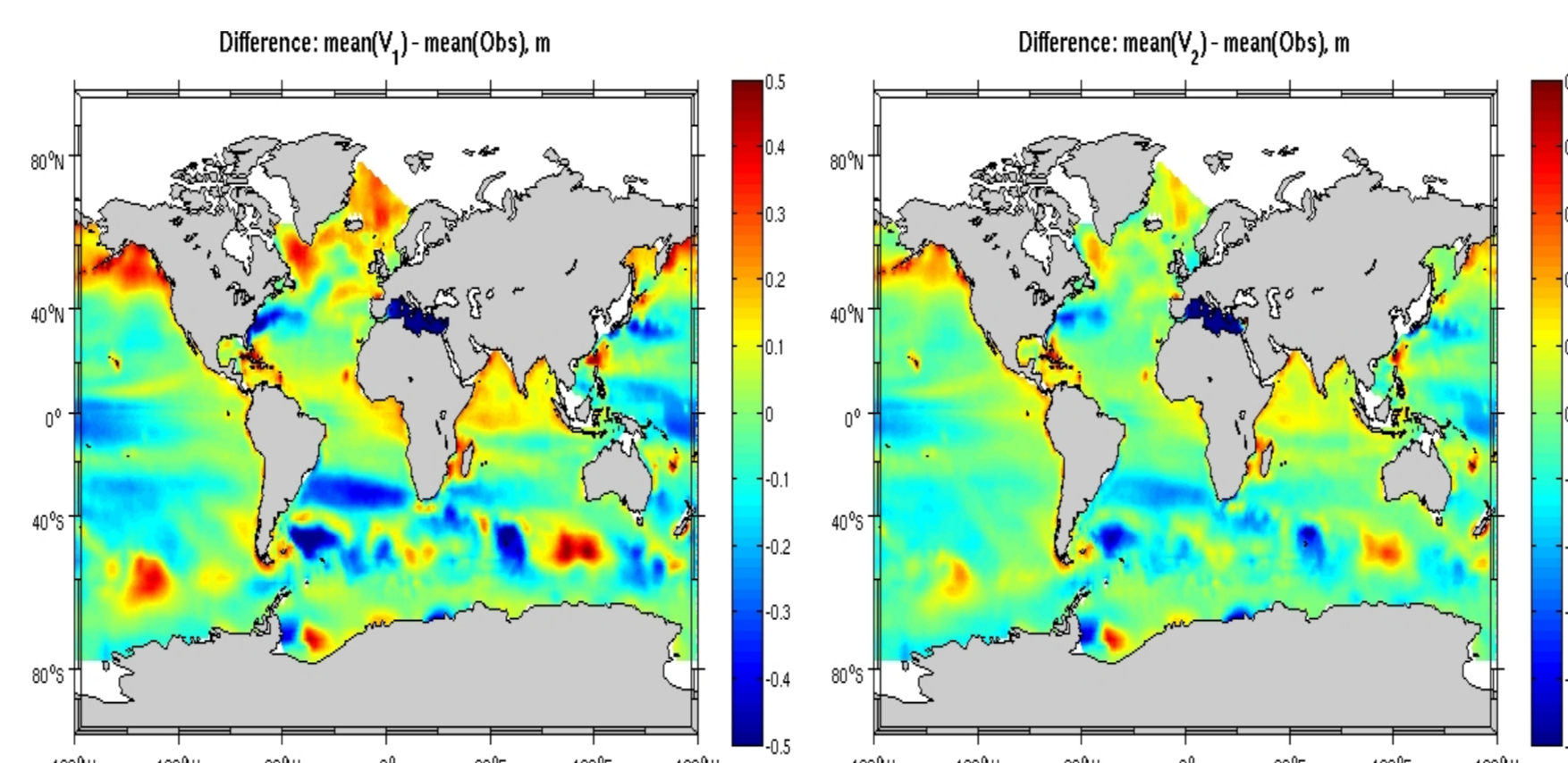
The difference is significant reaching ± 0.5 m in some areas. Many of them develop as the result of model adaptation to the bottom topography and present a systematic model bias.

The strong systematic difference between the observations and the model can be reduced by the adiabatic pressure correction suggested by [7, 2]. It works through modifying the pressure field leaving consistent tracer fields. It is introduced by replacing the model density ρ_m with a combination

$$\rho^* = \alpha \rho_m + (1 - \alpha) \rho_c$$

with $\alpha = 0.5$ and ρ_c the climatological density. The configuration of the model with this correction is further referred as V_2 .

The right panel of figure below shows mean difference calculated using V_2 configuration. The difference in the mean fields is reduced compared to the V_1 version in all regions, especially in North Atlantic.



Left: The mean difference between the DOT and model run V_1 .

Right: The mean difference between DOT and model run V_2 .

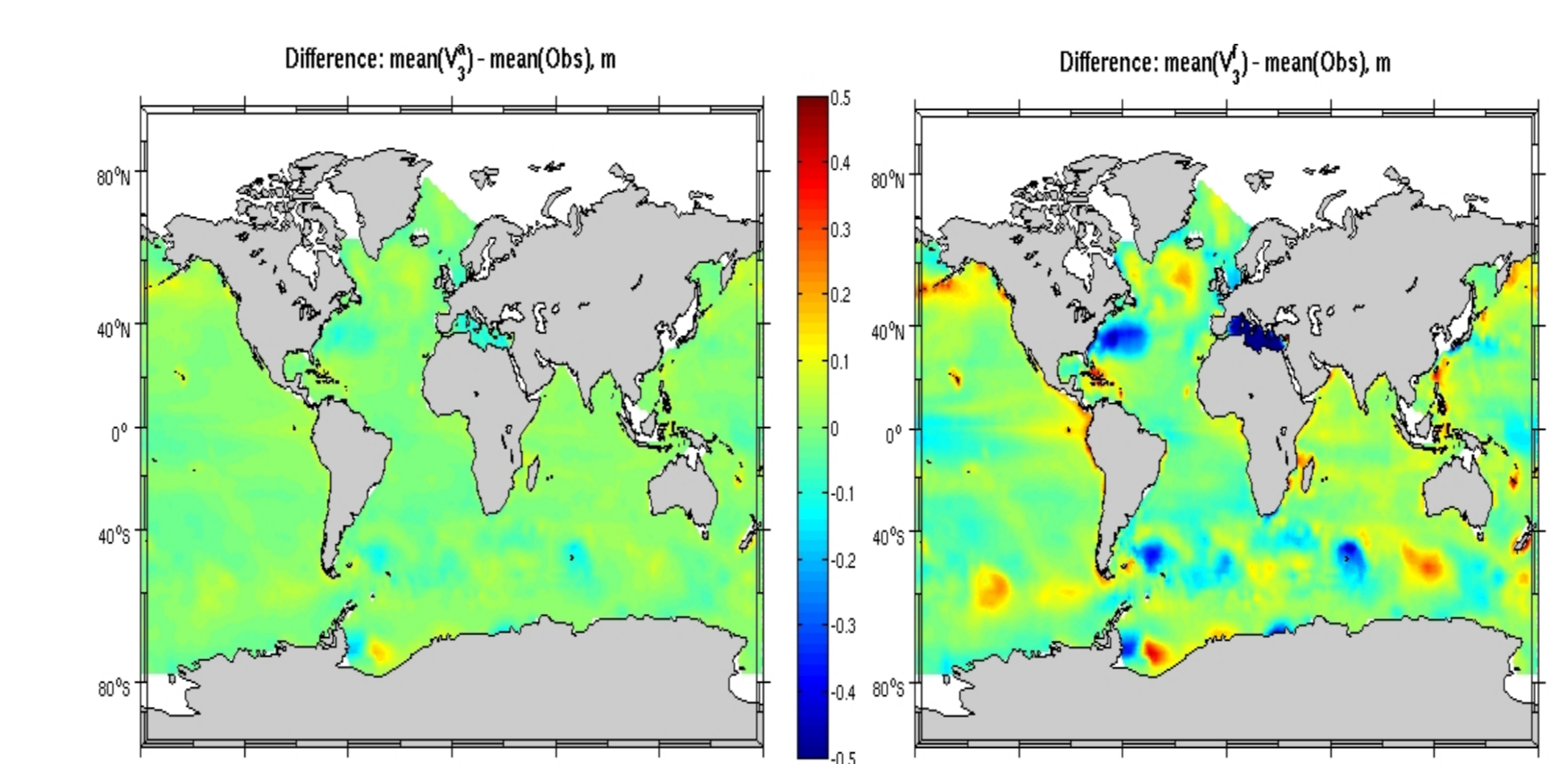
5 Assimilation scheme I

It is based on a model configuration V_2 . At each time the observations are available, the analysis of the SSH field is carried out applying the local SEIK filter [5] so that the analysis for each water column of the model depends only on observations within a specified influence region. In this study, the influence region is a circle with a radius of 200 km. Using this information, the vertical profiles of temperature and salinity are updated according to the vertical structure of the first baroclinic mode [3] with the amplitude computed from the elevation update, i.e.:

$$T^a(x, y, z) = T^f(x, y, z) + \delta\eta(x, y) \frac{g\rho_0 \hat{h}(z) \partial \bar{T}}{\hat{\rho}(0) \partial z}(x, y),$$

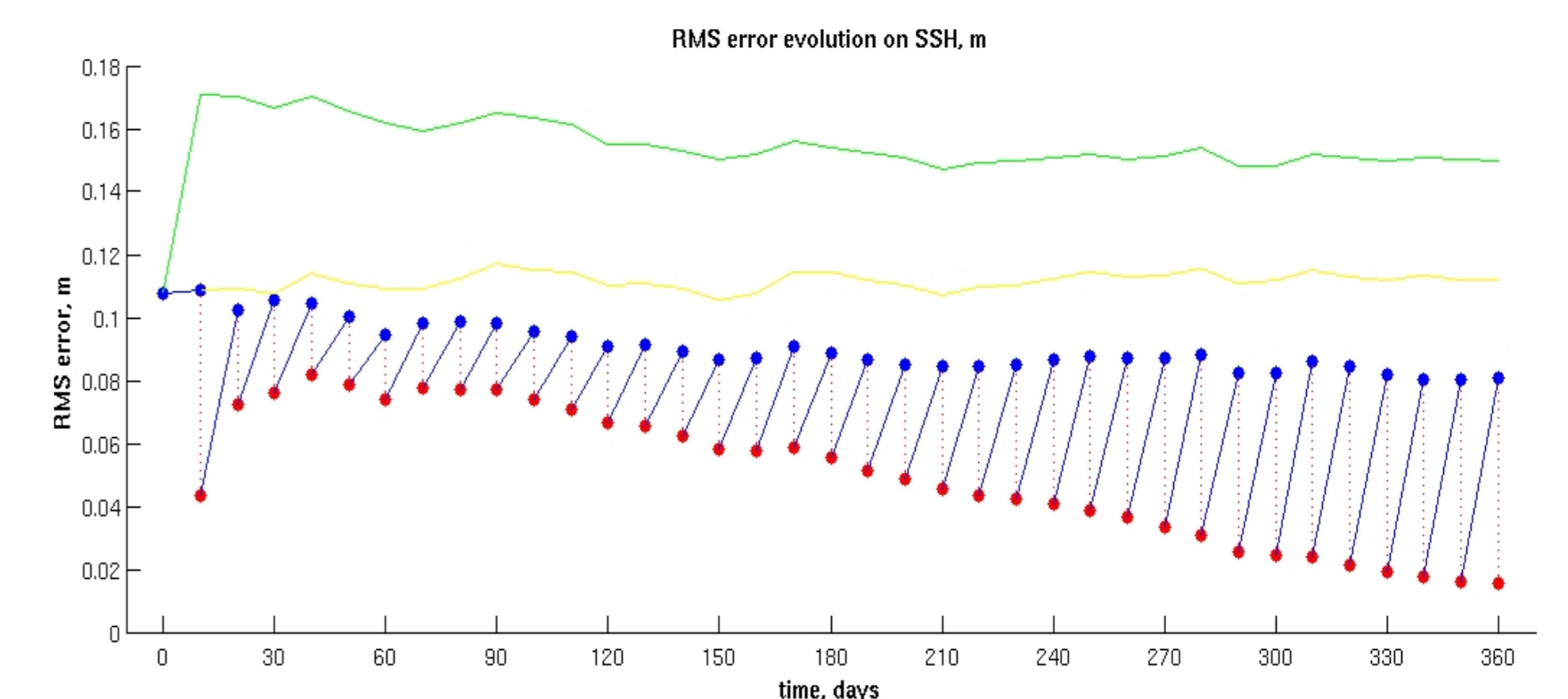
$$S^a(x, y, z) = S^f(x, y, z) + \delta\eta(x, y) \frac{g\rho_0 \hat{h}(z) \partial \bar{S}}{\hat{\rho}(0) \partial z}(x, y).$$

Here, overbars denote the reference state calculated as a mean from the one year free model run of the V_2 model, $\hat{\rho}$ and \hat{h} are locally defined vertical structures of the first baroclinic modes of velocity and displacement calculated using the local vertical profiles of the Brunt-Väisälä frequency and density from the V_2 model. The function $\delta\eta(x, y)$ is the analysis increment, i.e. the difference between the analysis of SSH, η_k^a and its forecast η_k^f , and g is the acceleration due to gravity. The velocity field is left unchanged so that it is simply the result of the model evolution.



Left: The mean difference between the dynamical topography obtained from the observations and from analysis.

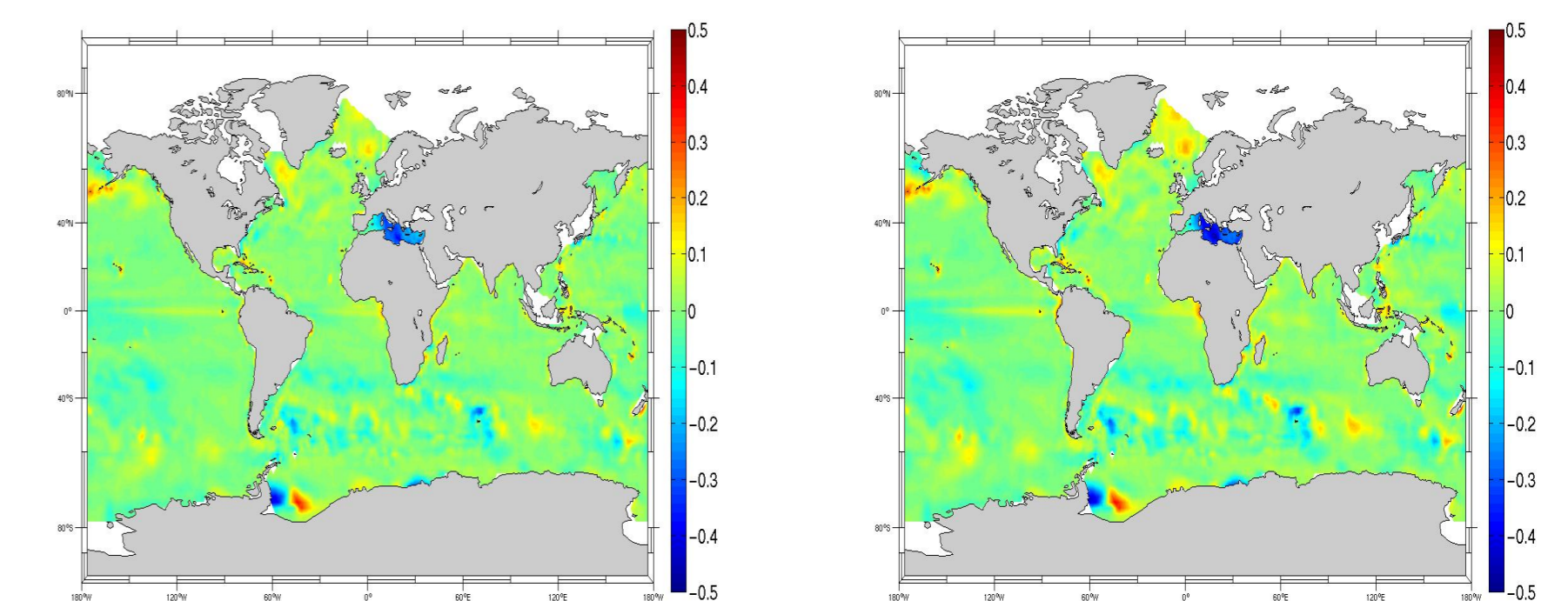
Right: The mean difference between the dynamical topography obtained from the observations and from forecasted fields.



Evolution of RMS error of SSH for the world ocean (except zones corresponding to RIO05 MDT location in the data). The green and yellow solid lines show the errors corresponding to the V_1 and V_2 free simulations (without assimilation), respectively. The blue lines with bullets represent the 10-day model forecasts, while the dotted red lines correspond to the analysis.

6 Assimilation scheme II

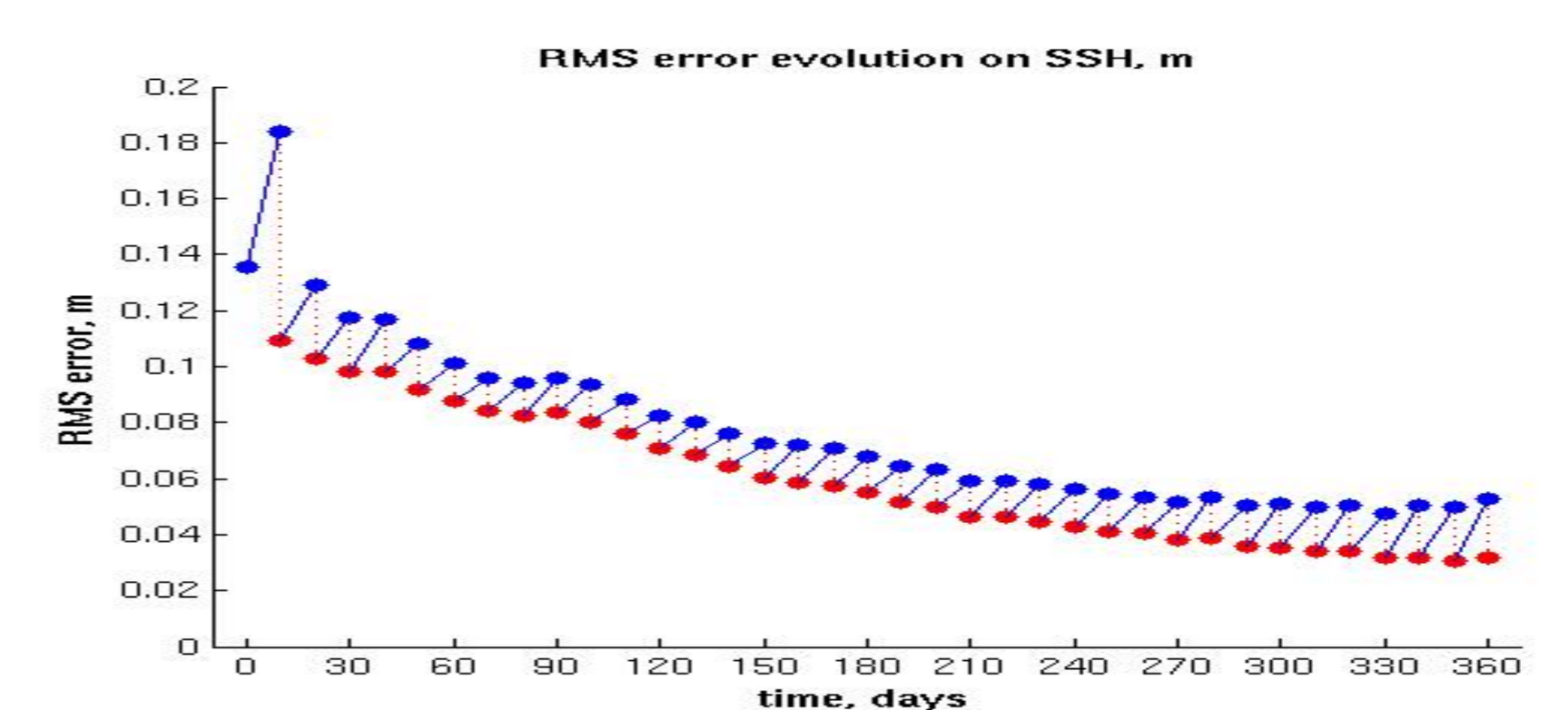
This assimilation experiment is based on a model configuration without the adiabatic pressure correction. At each time the observations are available, the analysis of the full ocean field is carried out applying the local SEIK filter [5] so that the analysis for each water column of the model depends only on observations within a specified influence region. In this experiment, the influence region is a circle with a radius of 900 km. The observational error covariance matrix is modified according to the distance of the observations to the water column using the 5th order polynomial weighting.



Experiment with 5th order polynomial weighting and $L = 9 \times 10^5$.

Left: The mean difference between DOT and analysis.

Right: The mean difference between DOT and forecasted fields.



Evolution of RMS error of SSH for the world ocean (except zones corresponding to RIO05 MDT location in the data) for assimilation scheme II.

7 Conclusion

- First assimilation technique leads to a partially successful assimilation approach reducing the rms difference between the model and data from 16 cm to 2 cm. However, it remains sub-optimal, showing a tendency in the forecast phase of returning toward a free run without data assimilation.
- Second assimilation technique leads to reduction of the rms difference between the model and data from 16 cm to 3 cm. Further, the tendency to return toward the free run is reduced for this technique.
- Both the mean difference and standard deviation of the difference between the forecast and observation data are reduced as the result of assimilation with sequential assimilation methods.

References

- [1] S. DANILOV and G. KIVMAN and J. SCHRÖTER (2004): A finite-element ocean model: principles and evaluation, *Ocean Modelling*, **6**, 125–150.
- [2] C. EDEN and R. GREATBATCH (2003): Adiabatically Correcting an Eddy-Permitting Model Using Large-Scale Hydrographic Data: Application to the Gulf Stream and the North Atlantic Current, *J. Phys. Oceanogr.*, **34**, 701–719.
- [3] I. FUKUMORI and R. RAUGHNATH and L. FU and Y. CHAO (1999): Assimilation of TOPEX/Poseidon altimeter data into a global ocean circulation model: How good are the results?, *J. Geophys. Res.*, **104**, 25 64725 665.
- [4] Q. WANG and S. DANILOV and J. SCHRÖTER (2008): Ocean circulation Model based on triangular prismatic elements with application in studying the effect of topography representation, *JGR*, **113**, C05015.
- [5] L. NERGER and S. DANILOV and W. HILLER and J. SCHRÖTER (2006): Using sea level data to constrain a finite-element primitive-equation ocean model with a local SEIK filter, *Ocean Dynamics*, **56**, 634–649.
- [6] L. NERGER and L., W. HILLER and J. SCHRÖTER (2005): PDAF - the Parallel Data Assimilation Framework: Experiences with Kalman filtering. In W. Zwielfhofer and G. Mozdzyński, editors, *Use of High Performance Computing in Meteorology - Proceedings of the 11. ECMWF Workshop*, pages 63–83. World Scientific.
- [7] J. SHENG and R.J. GREATBATCH and D. WRIGHT (2001): Improving the utility of ocean circulation models through adjustment of the momentum balance, *JGR*, **106**, 16711–16728.